JEE Journal of Ecological Engineering

Journal of Ecological Engineering 2022, 23(11), 109–121
https://doi.org/10.12911/22998993/153567
ISSN 2299–8993, License CC-BY 4.0

Received: 2022.08.15
Accepted: 2022.09.15
Published: 2022.10.01

Zeolitization of Coal Fly Ashes and Coal Fly Ash Microspheres

Katarzyna Rychlewska[1*], Martyna Tomaszewicz[2], Tomasz Radko[1]

[1] Institute of Energy and Fuel Processing Technology, ul. Zamkowa 1, 41-803 Zabrze, Poland

[2] Synthos S.A., ul. Chemików 1, 32-600 Oświęcim, Poland

* Corresponding author's e-mail: krychlewska@itpe.pl

ABSTRACT

The research investigated the efficiency of zeolitization of silicon and alumina bearing combustion by-products, i.e. coal fly ash and coal microspheres. Lab-scale alkali activation with 3M sodium hydroxide solution of raw materials obtained from a Polish coal-fired power plant were conducted at 100 °C. The obtained result proved that both combustion by-products are prone to zeolitization under the tested conditions with the obtained zeolite yields of 60 and 55% in the case of fly ash and microspheres, respectively. The main identified zeolite in the case of both by-products was NaP1.

Keywords: coal combustion by-products, zeolites, fly ash, fly ash microsphere.

INTRODUCTION

The production of electricity and/or heat in solid fuels-fired plants is inevitably associated with the formation of significant amounts of solid residues. Nevertheless, slags, fly and bottom ashes, as well as flue gas desulphurization wastes, formed as a result of coal combustion processes, are more and more often considered combustion by-products (CBP), rather than waste. Currently, due to their pozzolanic properties, coal combustion fly ashes are reused mainly in the building and construction sector as a concrete additive, in the mining industry for underground mine backfilling or in agriculture as soil liming agents and fertilizers [Uliasz-Bocheńczyk et al., 2015; Uzarowicz et al., 2015; Vilakazi et al., 2022]. In order to standardize the procedures for recognizing solid fuel combustion wastes as a by-product, facilitating the reuse of those wastes, a draft regulation of the Minister of Climate and Environment on the determination of detailed conditions for the loss of waste status for waste generated in the process of energy combustion of fuels [MKiŚ, 2021] was proposed in 2021. On the other hand, coal combustion microspheres, due to their properties, on the industrial scale are utilized mainly in the construction materials industry as performance improving fillers [Wajda et al., 2015]. Moreover, seeking for new directions of combustion by-products reuse is highlighted in Poland's Roadmap towards the Transition to the Circular Economy. One of such examples of turning those wastes into value-added products are synthetic zeolites, which are proven and very promising, as well as environmental-friendly direction of solid fuel combustion by-products upcycling. Zeolites are microporous hydrated aluminosilicates of alkali metals, alkaline earth metals or other cations [Wise, 2013]. The specific crystal structure of synthetic zeolites, inducing those resulting from combustion by-products reuse, containing numerous channels and chambers of various sizes, gives them a number of characteristic sorption, ion exchange, molecular-sieve and catalytic properties [Adamczyk et al., 2011; Czuma et al., 2019; Ren et al., 2020].

The formation of zeolites is a complex process, which involves the transformation of silicates and aluminates, the formation and dissolution of aluminosilicate, the continuous change in the gel's solid and solution phases, and the formation and growth of zeolite crystals. On the basis of changes in solid and liquid phases during synthesis, solid-phase, liquid-phase, and bidirectional

transformation mechanisms have been proposed [Ren et al., 2020]. According to the research data presented in the literature regarding coal fly (CFA) and bottom ash (CBA) zeolitization, zeolites like NaP1 (GIS) [Derkowski et al., 2006; Um et al., 2009; Czuma et al., 2019], NaA (LTA) [Wang et al., 2008; Xu et al., 2017; Amoni et al., 2022], sodalite/hydroxysodalite (SOD) [Hong et al., 2017; Shabani et al., 2019], CAN [Hong et al., 2017], 4A [Hui et al., 2006], MOR [Aono et al., 2018; Lankapati et al., 2020; Zhou et al., 2021], ZSM-5 [Zhu et al., 2014; Missengue et al., 2017; Feng et al., 2019], filipsite [Ceder *et al.*, 2018], FAU-type (NaX, NaY) [Derkowski et al., 2006; Padhy et al., 2015; Hu et al., 2017; Kunecki et al., 2017; Kurniawan et al., 2018; Sivalingam et al., 2018] and SSZ-13 [Gollakota et al., 2021] can be synthesized. Furthermore, zeolites materials and geopolymer/zeolite composites, containing zeolites like FAU [Liu et al., 2016; Liu et al., 2016], HS and NaX [Bertolini et al., 2013; Król et al., 2017] and Li-ABW [He et al., 2020] have been also prepared from CFA geopolymers by hydrothermal synthesis.

As part of the work, the possibility of using combustion by-products (fly ash and microspheres) in the process of zeolite synthesis by simple one-step alkaline activation method was investigated. The obtained zeolite materials were analysed in terms of type and amount of formed zeolites. According to the authors' knowledge, the presented results constitute a significant contribution to the research on the zeolitization of coal combustion microspheres, which topic is still poorly recognized.

METHODS ANS MATERIALS

Materials

For zeolitization purpose, two samples of coal combustion by-products, i.e., coal fly ash class A from pulverized coal combustion (waste code 10 01 02) and coal fly ash microspheres (waste code 10 01 81) were used. The samples were obtained from one of the Polish power stations powered by hard coal.

Characterization methods

The detailed characteristics of the physicochemical properties of the combustion by-products used in zeolitization included the chemical composition, particle size distributions and BET specific surface area. The chemical composition (oxide composition) of both by-products samples was determined by the Thermo Scientific ARL OPTIM'X wavelength dispersive x-ray fluorescence (WD-XRF) spectrometer. The phase composition of zeolitization products was determined with the powder X-ray diffraction method (XRD) using a PANalytical X'pert Pro MPD diffractometer (Theta-theta, PW 3040/60 Goniometer), with Cu anode lamp and X'Celerator detector. The analysis was performed within the angle range of 2.5 – 65 °2Θ. XRD measurements were conducted in the Bragg-Brentano geometry. The morphology of zeolitization products was analysed by Philips XL 30 ESEM environmental scanning electron microscope with the EDS X-ray microanalyzer by EDAX. Tests were carried out in a high vacuum mode with an accelerating voltage of 15 keV. Mainly the BSE (backscattered electron) detector was used for the research, showing, apart from the particle morphology, the differentiation of the chemical composition. Sometimes, for better visualization of morphology, mixed SEM/BSE images were also recorded. Chemical EDS microanalyses were performed at selected points of samples. The samples were prepared by applying the thin layer of ground powder to the adhesive carbon substrate placed on the aluminium stage and spraying with coal. The specific surface area of starting materials and obtained zeolites was determined based on the nitrogen vapour adsorption and desorption curves at the temperature of 77 K (Micromeritics 3Flex Adsorption Analyzer). The BET specific surface values were calculated using the ISO 9277:2010 standard.

Zeolite hydrothermal synthesis

In order to experimentally verify the efficiency of both combustion by-products zeolitization, a laboratory set-up was assembled (Fig. 1). It consisted of a glycerine bath placed on the heating magnetic stirrer and the temperature control system. A round-bottom flask with a reflux condenser was placed in the bath. Such arrangement allowed the temperature and the amount of water in the reaction flask to be kept constant.

The general scheme of the adopted zeolitization procedure, developed based on the literature review, is shown in Fig. 2. The adopted method was single-step direct alkali activation treatment

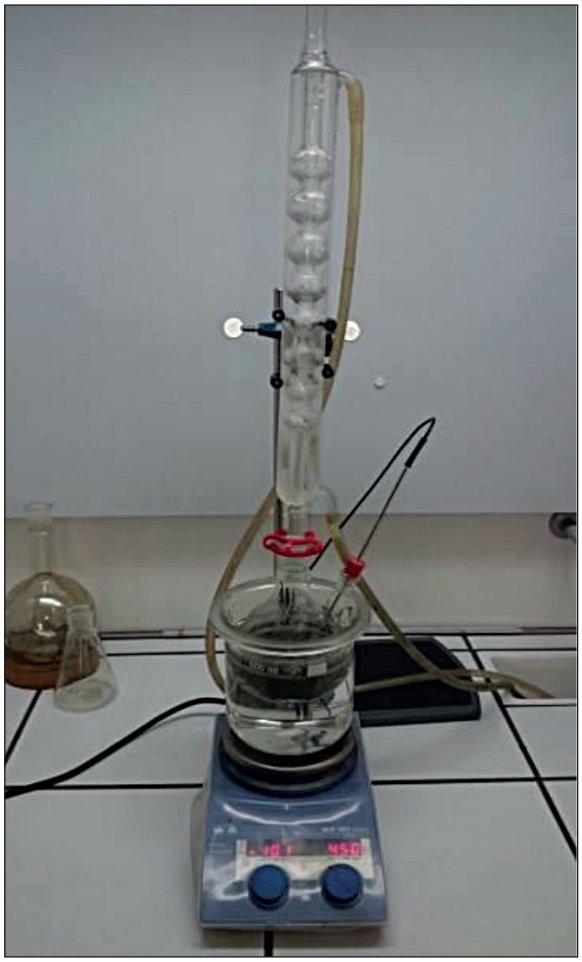

Figure 1. Laboratory set-up for the zeolitization of combustion by-products

at atmospheric pressure. Both by-products were subjected to one-step hydrothermal synthesis without previous alkali fusion or sonification, which increase the reactivity and accessibility of silicon and aluminium but are associated with the increase in the energy demand.

In the prepared laboratory set-up, 4 experiments were carried out in which the 12.5 g fly ash or coal microspheres was treated with 150 cm^3 of 3M solution of sodium hydroxide (solid to liquid ratio of 83.3 g/dm^3) at the temperature of 100°C for 6, 24 and 48 hours, while microspheres – at 100° C for 24 hours. All experiments were carried out without adding the external Si and Al sources. The zeolitization products were washed on the filter to remove sodium hydroxide and dried. After drying, the samples were subjected to XRD, SEM, and specific surface area analyses.

RESULTS AND DISCUSSION

Raw material composition

According to the XRF results (Table 1), the major compounds in both tested coal combustion by-products samples include SiO_2, Al_2O_3 and Fe_2O_3. Minor compounds include Na_2O, P_2O_5, SO_3, TiO_2, CaO, K_2O, and MgO and MnO. The Si/Al weight ratios of the examined fly ash and microspheres were 2.02 and 1.85, respectively.

Phase composition of zeolitization products

The samples obtained as a result of a 24-hour leaching of fly ash (Z1) and microspheres (Z2) were subjected to X-ray examinations in order to determine the phase composition. Diffractograms of the tested samples are presented in Figs. 3 and 4. On the basis of the phase composition analysis

Table 1. Chemical compositions of coal fly ash and fly ash microspheres

wt. %	Chemical composition of coal fly ash and microspheres	
	Fly ash	Fly ash microspheres
SiO_2	51.80	55.07
Al_2O_3	26.82	34.14
Fe_2O_3	7.01	1.54
CaO	3.41	0.98
K_2O	2.88	0.60
MgO	2.41	0.38
Na_2O	1.35	0.56
TiO_2	1.27	1.07
P_2O_5	0.40	0.51
SO_3	0.64	0.13
Mn_3O_4	0.08	0.04
BaO	0.13	0.17
SrO	0.06	0.06
LOI	3.2	0.8

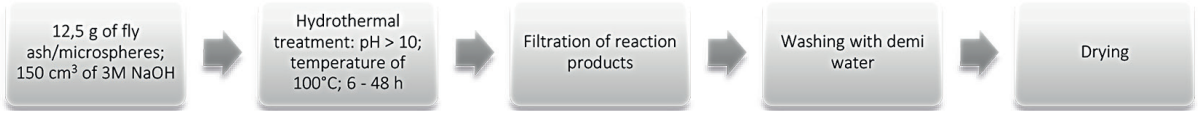

Figure 2. Schematic diagram of lab-scale zeolitization process

of the synthesized materials, it was found that the total zeolite yield in the case of the Z1 sample was approx. 63%, while in the case of the Z2 – approx. 55%. The main zeolite phases identified in the Z1 sample (Fig. 3) was Na-exchanged Zeolite P1 (the best fit is shown in pattern # 98-000-9550 of the ICSD base (2015)), the synthetic analogue of the gismondine-type (GIS-type) zeolites with formula $Na_6Al_6Si_{10}O_{32}12H_2O$. In the case of the Z1 sample, the diffraction pattern shows all diagnostic reflections, and the match according to the "score" indicator to the pattern was 63%. The strongest reflections of NaP1 phase were 7.09 Å and 3.174 Å, while the following were also very well visible: 5.013 Å; 4.105 Å and 2.686 Å. The content of identified NaP1 zeolite in the Z1 sample, calculated by the Rietveld method, was about 60%.

Content of other zeolite phases, i.e., zeolite A (synthetic LTA zeolite; pattern # 98-020-1050) with a main reflex of 12.20 Å and Na-X zeolite (synthetic faujasite-FAU zeolite; pattern # 98-015-5683) with a major reflex of 14.34 Å, were much smaller and only the most intense mentioned reflections were observed. Furthermore, in the Z1 sample, a sulphate-bearing sodalite-type zeolite phase was also observed. Apart from zeolite minerals, The Z1 sample was also characterized by the high amount of unreacted mullite and a small amount of quartz. The quantitative and qualitative composition of the Z1 sample was NaP1 zeolite – 59.2 wt.%, mullite – 30.4 wt.%, quartz – 7.0 wt.%, Zeolite A – 1.5 wt.%, Sodalite – 1.7 wt.% and the NaX zeolite – 0.2 wt.%. According to the literature data, the NaP1 zeolite is one the most frequently observed products of coal fly and bottom ash direct single-step zeolitization. Studies on different zeolites phase synthesis from coal fly ashes, conducted by Derkowski and coworkers [Derkowski et al., 2007] suggest that crystallization of NaP1 phases took place during reactions at high temperatures (150°C) and under the low NaOH concentrations (0.5M). The presence of Cl^- was not critical since the EDS data indicated, that Cl^- was absent in the structure of the NaP1 synthesized with NaCl added. Literature data indicates that NaP1 crystallization took place from a solution of higher Si content than required by other zeolites typically observed in combustion by-products alkali activation, namely FAU-type, SOD and CAN. This is consistent with the fact, that the Si/Al molar ratio of NaP1 is the highest among all mentioned zeolites. The experiments by Hollman et al. [Hollman et al., 1999], who synthesized various zeolites at 90°C using two-step hydrothermal method by reacting fly ash extraction liquor with 2M NaOH solution indicated that the NaA (+ some amount of sodalite) phase crystallized in a solution with Si/Al = 1.2, NaX in a solution with Si/Al = 1.8 and NaP1 commenced its growth in solution with Si/Al = 2.0. The results presented by Inada [Inada et al., 2005] on the effect of Si/Al molar ratio on the type of formed zeolite (100°C; particle size of the fly ash was 0.5–100 µm; solid/liquid ratio of 125 g/

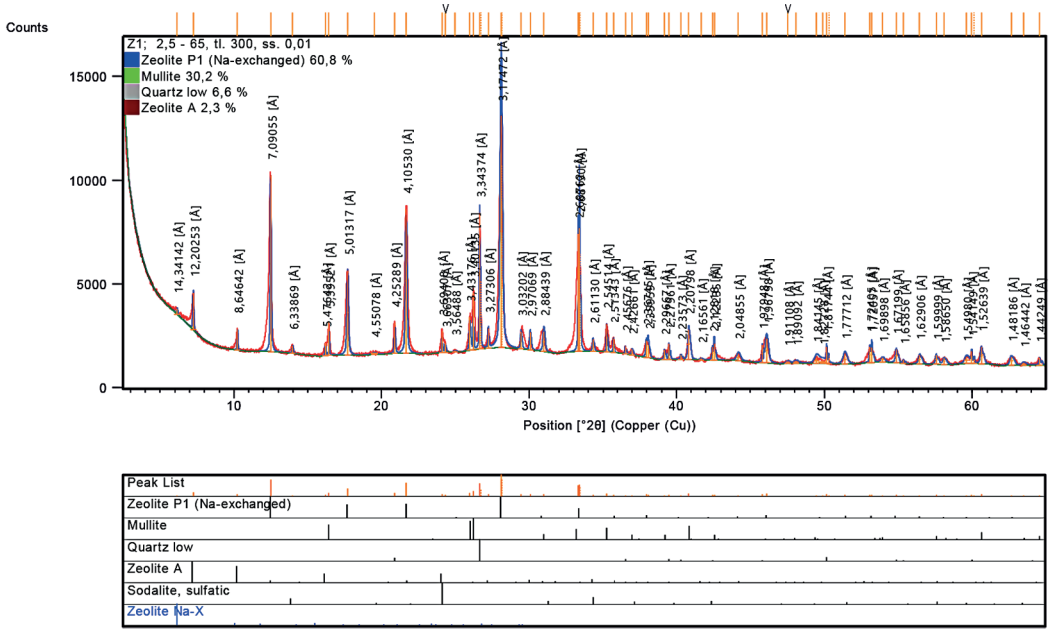

Figure 3. X-ray powder diffraction of sample Z1

dm^3; 24 h) confirmed that the high-Si concentration and low-Al concentration are the factors for forming zeolite NaP1, which was predominantly formed from silica-rich fly ash at a lower NaOH concentration (1-2M NaOH). Hydroxy-sodalite (SOD) has the larger amount of Al than the NaP1 zeolite, so it was apt to form when the Al dissolution was enhanced at the higher NaOH concentration (> 3.5M). Nevertheless, it was found that silica addition effectively enhances the formation of zeolite NaP1, even at a high NaOH concentration. Taking into account the observed relationships described above, it can be concluded that the relatively high content of NaP1 zeolite in the obtained product resulted from the application of relatively high-concentrated sodium hydroxide, which allowed increasing the amount of dissolved silicon in the synthesis solution.

Wałek and co-workers [Wałek et al., 2008] synthesized the single phase NaP1 zeolite with 80 wt.% crystallinity (Na-P1 zeolite and low intensity peaks of mullite and quartz were identified in the XRD pattern of the product obtained) from raw and ground Class F coal fly ash (Si/Al wt. ratio of 2.00) by the direct hydrothermal method with high temperature at the initial dissolution stage (104°C) and reduced temperature at the crystallization stage (80°C). The synthesis was carried out at S/L ratio of 4 g/dm^3 in 2M NaOH solution for 96 h. Na-P1 zeolite was also formed during the direct hydrothermal treatment of ground Class F and C coal fly ashes performed by Kunecki et al. (Kunecki *et al.*, 2021) – the synthesis was conducted at S/L ratio of 40 g/dm^3 and 105°C for 24 h in 400 cm^3 1M NaOH solution with the addition of 100 cm^3 of 3M NaCl and the best quality product resulted from the alkali treatment of highly grinded Class F ash (Si/Al wt. ratio of 1.95) with the characteristic Dx(10), Dx(50) and Dx(90) particles diameters of 5.09 μm, 24.20 μm and 104 μm, respectively. A direct hydrothermal method for the synthesis of NaP1 zeolite, along with analcime, from Polish fly ash derived from hard coal combustion in pulverized-fuel boilers was also proposed by Adamczyk [Adamczyk et al., 2005]. The zeolite synthesis was performed from Class F fly ash (Si/Al wt. ratio of 1.26), which were activated for 6 h with 1.16 M sodium hydroxide solution, liquid to solid ratio of 6:1 g/cm^3 (100 g of CFA in each experiment) and within the temperature range of 80 to 320°C. The NaP1 zeolite and analcime started to crystallize at 120°C. As the synthesis temperature increases to 200°C, the NaP1 type zeolite content raised, while analcime was present in the trace quantities. Traditional single-step direct hydrothermal treatment at the temperature of 90°C in 2M sodium hydroxide for 96 h at solid/liquid ratio of 400 g/dm^3 conducted by Hollman and co-workers [Hollman et al., 1999] yielded the product with 40–45 wt.% of NaP1 zeolite content. Um and others [Um et al., 2009] obtained the NaP1 zeolite from coal bottom ashes pre-treated by the density separation based on sink-float procedure and alkali activation of the fraction characterized by the lower specific gravity and higher content of amorphous aluminosilicate glass (2M NaOH; 120°C; S/L ratio of approx. 166.7 g/dm^3; 24 h). The authors did not report on the formation of other zeolite phases; nevertheless, the synthesized product contained some amount of unreacted quartz. Derkowski and others [Derkowski et al., 2006] synthesized the zeolitic material containing NaP1 zeolite by simple direct method – 10 g of CFA (Si/Al weight ratio of 1.66) was activated using mixture of 200 cm^3 of 1M NaOH and 100 cm^3 of 3M NaCl solution (S/L ratio approx. 33.3 g/dm^3) for 24 h in 105°C and under atmospheric pressure. The obtained zeolite material was abundant in NaP1 zeolite, while mullite and quartz occurred in the amounts that seem to be not significantly different from the contents in the raw fly ash. A small content of an amorphous substance was noticed due to the slight rise of the background line in the XRD pattern. Trace amount of sodalite (SOD) was also detected in by XRD. Cardoso et al. [Cardoso et al., 2015] synthesized the zeolite material containing 77 wt.% of NaP1 zeolite with some minor amount of analcime from coal fly ash characterized by high Si/Al weight ratio of 2.65, high content of amorphous phase (> 80 wt.%) and low content of mullite (< 7 wt.%). Before the synthesis, ash was partially purified from magnetic particles, which have been recognized as inhibiting the synthesis of zeolites by means of the dry separation. The synthesis was conducted in pressurized autoclave under autogenous pressure for 24 h in the presence of 1.0M NaOH solution in 150°C.

The Z2 sample, obtained during the alkali activation of coal combustion microspheres, was characterized by less diversified mineral (phase) composition (Fig. 4) and was dominated by three phases, i.e., NaP1 zeolite (55.5 wt.%), which was the only identified zeolite in the zeolitization product (the diffraction pattern of the Z2 sample presented in Fig. 6 lacks the characteristic

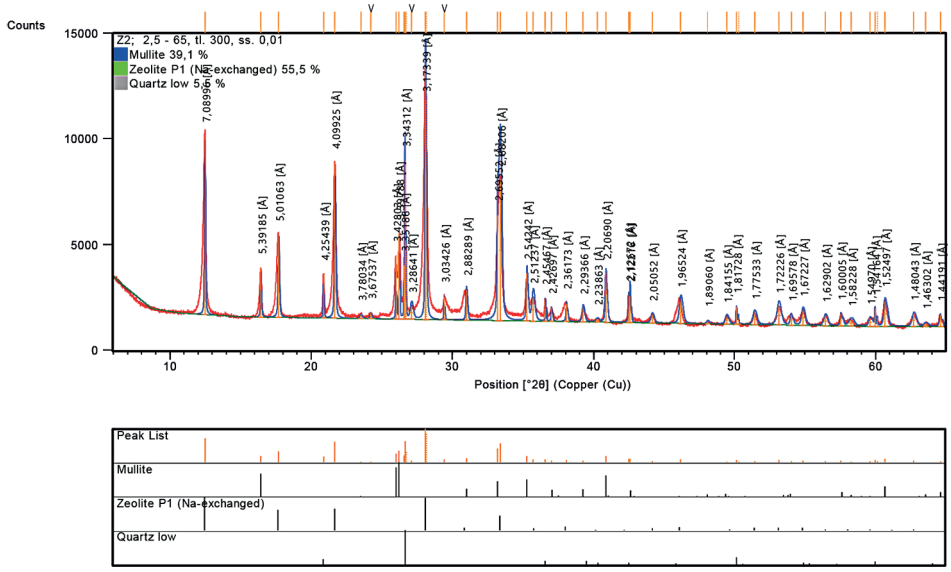

Figure 4. X-ray powder diffraction of sample Z2

reflections for other types of zeolites), as well as high amount of unreacted mullite (39.1 wt.%) and quartz – 5.4 wt.%. Similar results were obtained by Kunecki and others [Kunecki et al., 2018]. According to their studies on microspheres zeolitization, NaP1 zeolite appeared already after 4 h of the hydrothermal process (3M NaOH, 80°C and solid/liquid ratio of approx. 167 g/dm^3) and the largest amount of NaP1 zeolite was ascertained for the sample after 26 h of the conversion time. Pichór and co-workers [Pichór et al., 2014] conducted a series of experiments on coal fly ash microspheres zeolitization under different condition. According to the presented results, the NaP1 zeolite appeared as the product of microspheres alkali activation when synthesis was conducted under the 4–5M NaOH solution regardless of the reaction temperature (75 and 90°C) and time (48 and 72h).

Specific surface area analysis

As it can be seen in Tab.2, for the adopted conditions of direct hydrothermal synthesis of zeolites (3M NaOH solution, 100°C), after 6 hours of fly ash leaching, the specific surface area increased almost 10 times in comparison to the starting material, and in the case of 24 hours of leaching – a nearly 19-fold increase of the surface area was observed. Further extension of the hydrothermal alkali activation did not increase the surface area, but even slightly decreases it. The observed development of specific surface after 24 h of alkali activation in 105°C was higher than that obtained by Derkowski and others [Derkowski et al., 2006], which may be due to the use of a less concentrated sodium hydroxide solution (1M NaOH) mixture with 3M NaCl solution. The obtained values of S_{BET} correspond with the results of fly ash alkali activation conducted by Musyoka and co-workers [Musyoka, 2009; Musyoka et al., 2012] – after 24 h and 48 h of treatment in 140°C with, the S_{BET} of the tested fly ash increased to 58.64 m^2/g and 67.63 m^2/g, respectively. However, Musyoka applied the two-step hydrothermal synthesis enabling to produce higher-purity zeolites. Furthermore, the presented result correspond with the experimental data published by Woolard et al. [2000] – obtained zeolite material containing NaP1, resulting from direct hydrothermal activation of coal fly ash with 1M NaOH solution for 21 h, was characterized by S_{BET} of 62.66 m^2/g, while S_{BET} of raw CFA was 1.05 m^2/g.

When microspheres were used as the starting material, a 24-hours leaching resulted in a surface increase up to 44 times – from 0.84 m^2/g to 36.92 m^2/g. The obtained results correspond with the

Table 2. Comparison of the BET specific surface areas of starting materials and obtained zeolites

Time, h	BET specific surface area $S_{BET,}$ m^2/g	
	Fly ash	Fly ash microspheres
raw	3.52	0.84
6 h	34.9	-
24 h	66.81	36.92
48 h	63.00	-

experimental data presented by Kunecki and others [Kunecki et al., 2016; Kunecki et al., 2018] – although no data for raw microspheres were presented, nevertheless after 26-hours of synthesis, the obtained product was characterized by S_{BET} of 47.93 m^2/g. However, the absolute value of the specific surface area of the zeolite obtained from microspheres is nearly half that of the zeolite obtained from fly ash.

SEM/EDS analysis of obtained zeolite materials

The zeolite products resulting from the 24-hour hydrothermal treatment of fly ash (Z1) and microspheres (Z2) were also tested in terms of microstructure and chemical composition using the SEM/EDS technique coupled with BSE detector. To illustrate the morphology of obtained products, the SEM-BSE images of both samples were taken at 500× and 200× magnification (Fig. 5). It can be seen that both samples were composed of aggregates of spheres with a differential diameters. These aggregates resembled clusters and ranged in size from several to several dozen micrometres. Apart from aggregates, both samples contained single spheres (diameter of several to several dozen micrometres) and sharp-edged particles. Some of the particles in sample Z1 contained precipitation of iron oxides. Additionally, porous fragments of microspheres (original diameter of several hundred micrometres) appeared quite often in sample Z2.

As indicated by XRD analysis, the main non-zeolite components of sample Z1 included mullite and quartz. Mullite formed rod/acicular needle-like crystals, usually inside hollow particles composed of aluminosilicate glass (Fig. 6). Moreover, in sample Z1, small amounts of iron oxides precipitation of size of 1–2 micrometres were observed, usually on the outer surface of mullite particles (Fig. 7), as well as sharp-edged crystals having composition corresponding to quartz (Fig. 8). Radially needle-shaped submicron crystals, possibly natrolite,

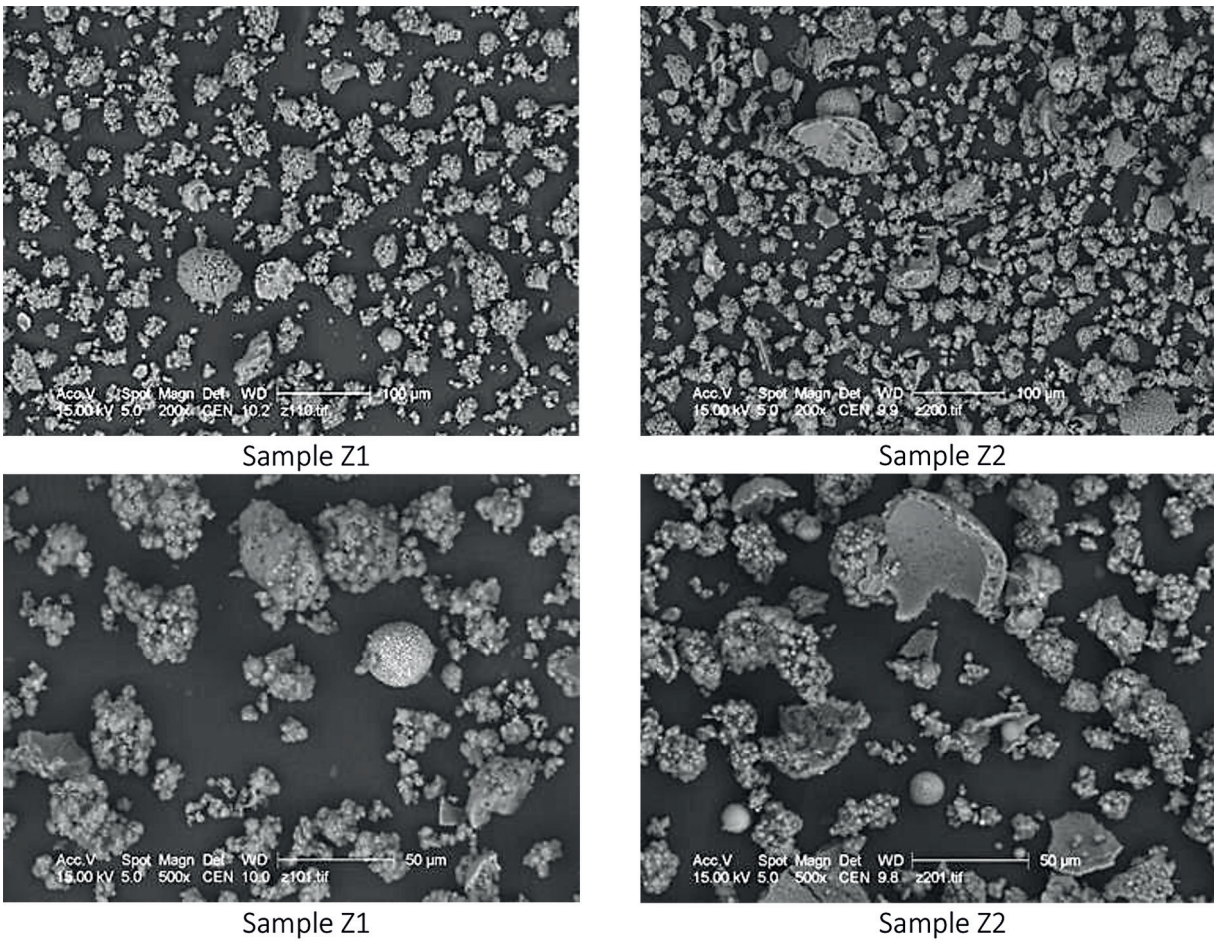

Figure 5. SEM-BSE images of synthesized zeolite materials (200-fold magnification – top and 500-fold magnification – down)

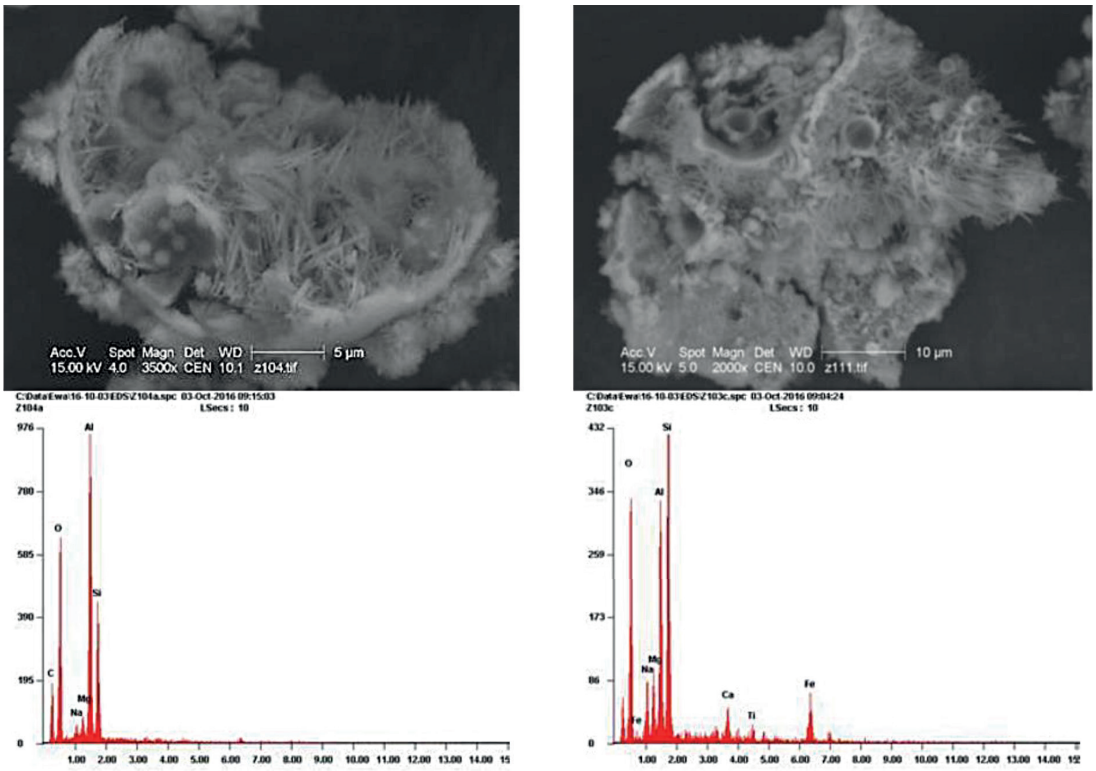

Figure 6. SEM-BSE images of rod/acicular needle-like mullite crystals on the inner surface of aluminosilicate glass (a, b) and EDS analysis of mullite (c) and aluminosilicate glass (d) in sample Z1

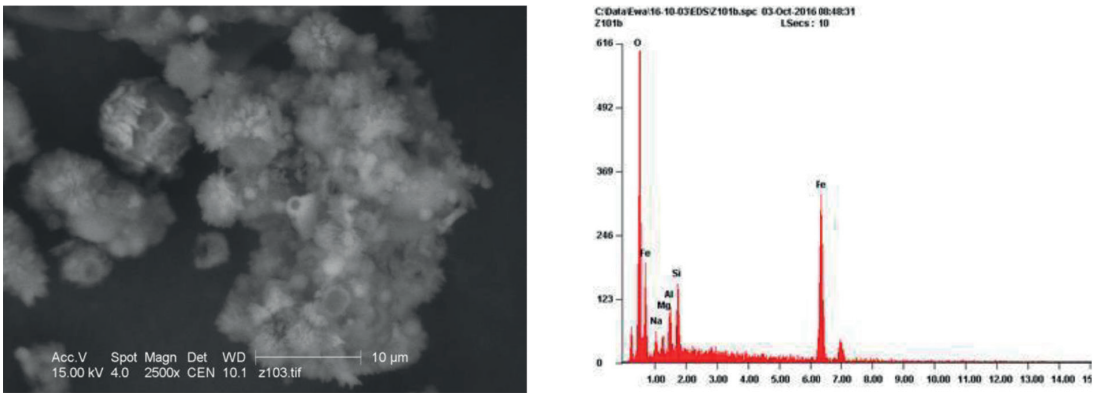

Figure 7. SEM-BSE images of mullite sphere with iron oxides precipitation and EDS spectrum of iron oxides in sample Z1

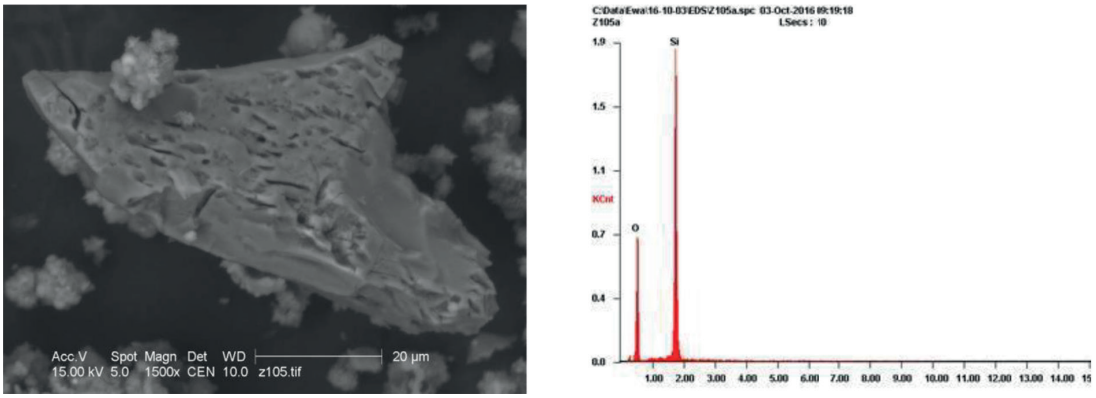

Figure 8. SEM-BSE images and EDS spectrum of quartz crystal in sample Z1

were also grown on the outer surface of the sodium aluminosilicate and mullite particles (Fig. 9). Similar to the Z1 sample, the Z2 sample consisted mainly of mullite, quartz and zeolite NaP1. Moreover, in the case of Z2, mullite formed rod/needle crystals inside the very fine (<1 μm) microspheres (Fig. 10). Furthermore, on the outer surface of the microspheres, acicular, submicron zeolite crystals,

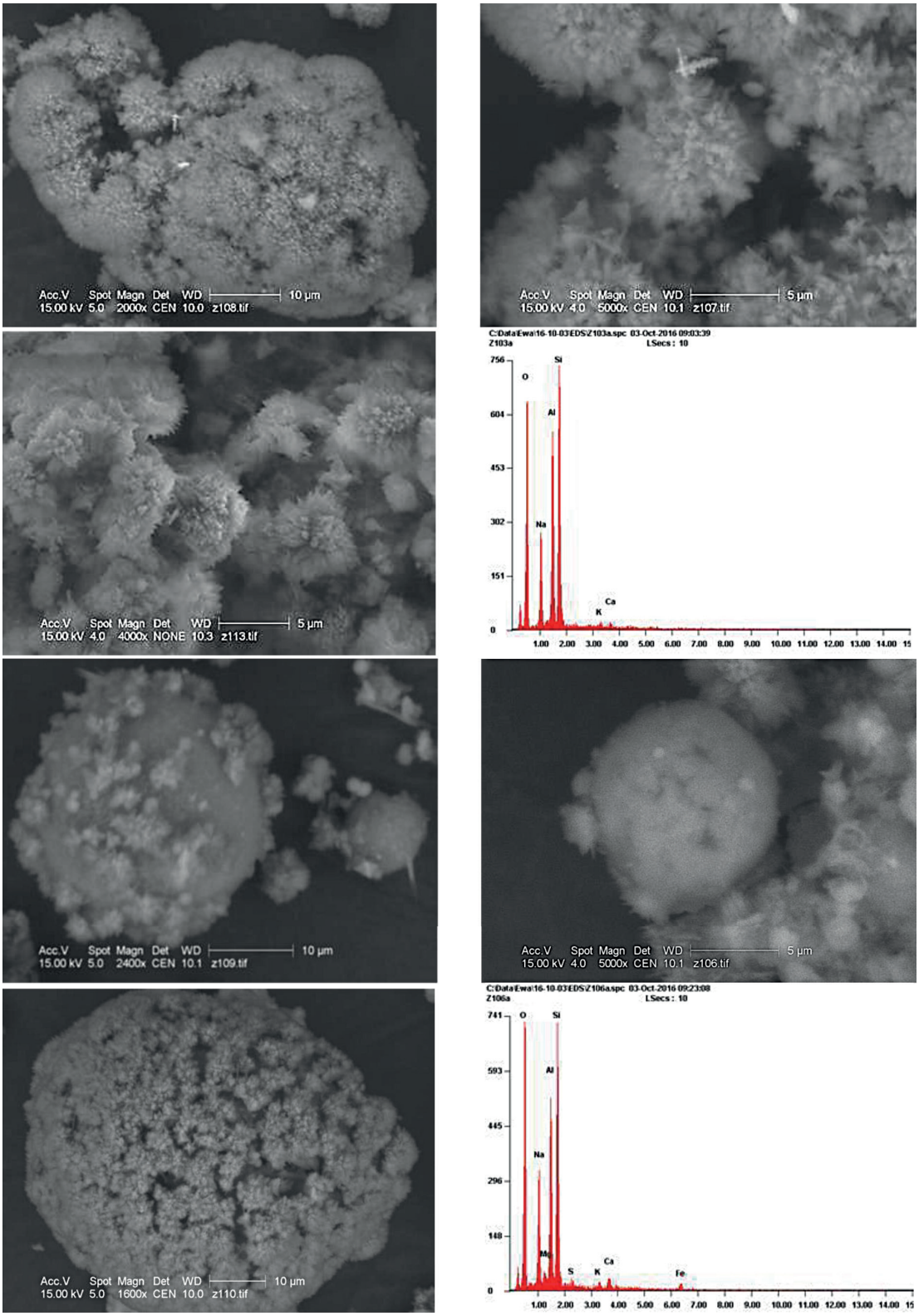

Figure 9. SEM-BSE images and EDS analysis of zeolite crystals on aluminosilicate (a, b, c, d) and mullite spheres (e, f, g, h) in sample Z1

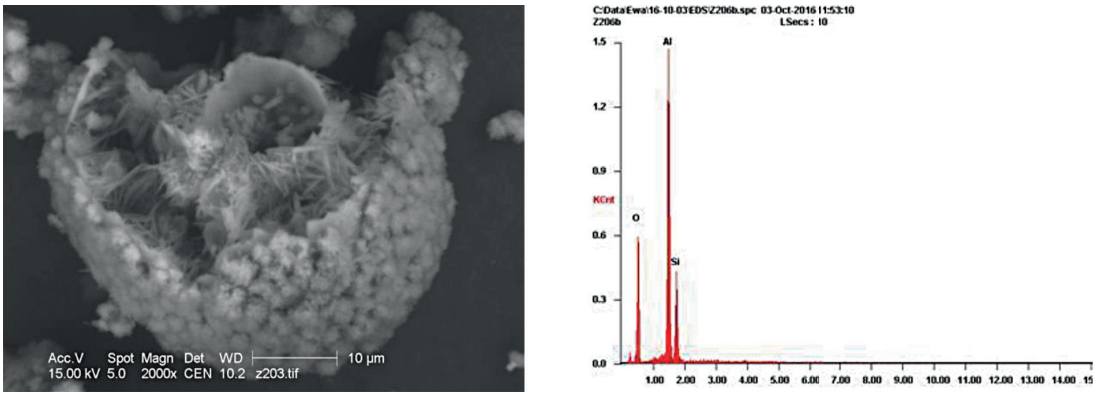

Figure 10. SEM-BSE images of rod/acicular needle-like mullite crystals on the inner surface of aluminosilicate glass and EDS spectrum of mullite in sample Z1

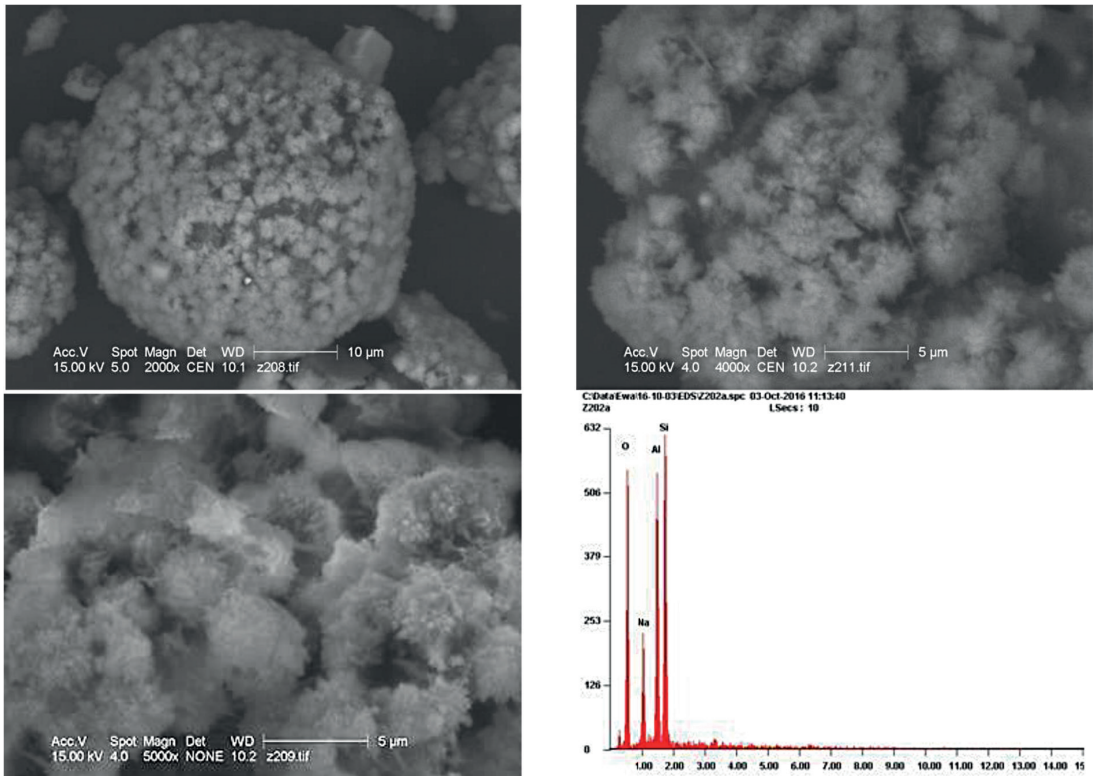

Figure 11. SEM-BSE images (a, b, c) and EDS (d) analysis of zeolite crystals formed on mullite spheres in sample Z2

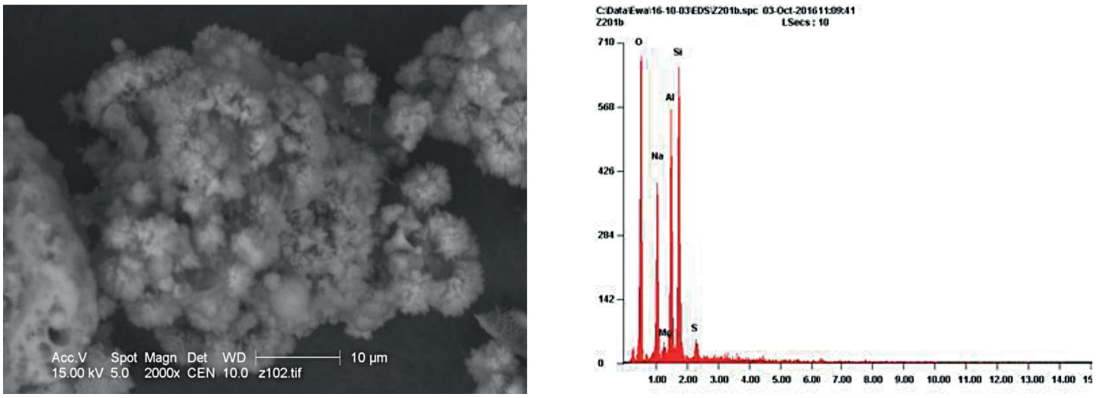

Figure 12. SEM-BSE images and EDS analysis of zeolite (sodalite) crystals formed on mullite spheres in sample Z2

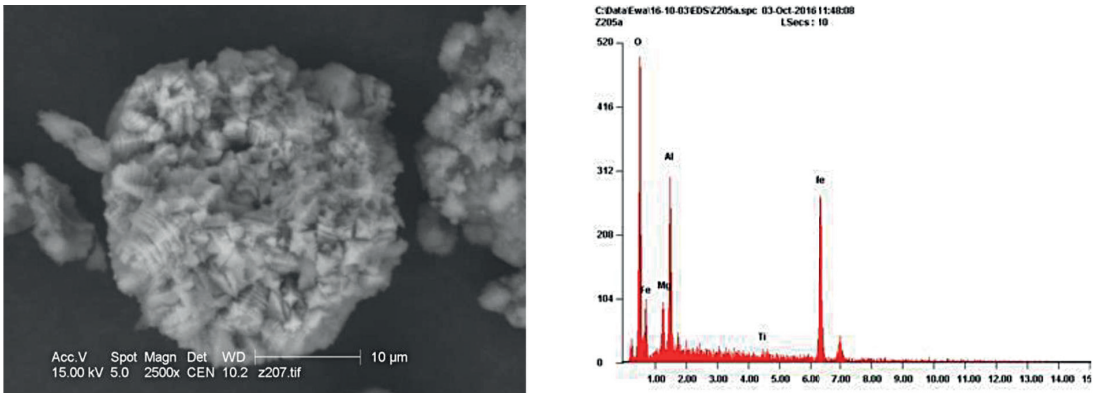

Figure 13. SEM-BSE images and EDS spectrum of aluminium, magnesium and iron oxides in sample Z2

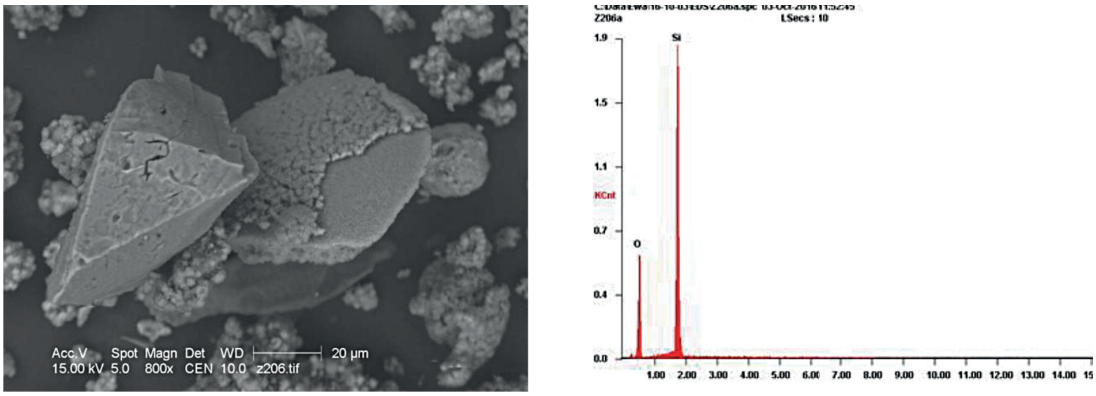

Figure 14. SEM-BSE images and EDS spectrum of quartz crystal in sample Z2

forming quite compact spheres, were observed (Fig. 11). Few of them were characterized by the increased content of sodium and contained the small amount of sulphur, which may indicate the zeolite from the sodalite group (Fig. 12). In addition, the sample contained aluminum, iron and magnesium oxides, forming crystals of several micrometres (Fig. 13), as well as the crystals corresponding to the composition of quartz (Fig. 14).

CONCLUSIONS

The obtained results demonstrated that the fly ash and fly ash microspheres from pulverized coal combustion in Polish power plant can be used as raw material in the synthesis of zeolite Na-P1, employing simple single-stage hydrothermal conversion. On the basis of the phase composition analysis of the synthesized materials, it was found that the total zeolite yield in the case of the Z1 sample was approx. 63%, while in the case of the Z2 – approx. 55%. The main zeolite phases identified in both samples was Na-exchanged Zeolite P1 (the best fit is shown in pattern # 98-000-9550 of the ICSD base (2015)), the synthetic analogue of the gismondine-type (GIS-type) zeolites with formula $Na_6Al_6Si_{10}O_{32}12H_2O$. 24-hour leaching of raw materials with the 3 M NaOH solution showed, that in the case of fly ash the surface development of zeolite occurred 10 times in relation to the raw material, while in the case of microspheres, the surface development was 44 times.

Acknowledgments

This work was performed with a financial support of the Ministry of Science and Higher Education under state subsidy project "Research on the study solid combustion by-products management processes, including a review of intellectual property rights" no 11.16.018.

REFERENCES

1. Adamczyk, Z., Białecka, B. 2005. Hydrothermal synthesis of zeolites from Polish coal fly ash. Polish Journal of Environmental Studies, 14(6), 713–719.
2. Adamczyk, Z., Gruchociak, E., Loska, K. 2011.

Sorption of heavy metals in synthetic zeolite type NaP1. Górnictwo i Geologia, 6(3), 5–12.

3. Amoni, B. C. et al. 2022. Effect of coal fly ash treatments on synthesis of high-quality zeolite A as a potential additive for warm mix asphalt. Materials Chemistry and Physics, 275, 125197.
4. Aono, H. et al. 2018. Cs + decontamination properties of mordenites and composite materials synthesized from coal fly ash and rice husk ash. Journal of Asian Ceramic Societies, 6(3), 213–221.
5. Bertolini, T.C.R. et al. 2013. Adsorption of Crystal Violet Dye from Aqueous Solution onto Zeolites from Coal Fly and Bottom Ashes. Orbital: the Electronic Journal of Chemistry, 5(3), 179–191.
6. Cardoso, A.M. et al. 2015. Synthesis of zeolite Na-P1 under mild conditions using Brazilian coal fly ash and its application in wastewater treatment. Fuel, 139, 59–67.
7. Ceder, J. et al. 2018. Synteza filipsytu z popiołów lotnych oraz jego potencjalne zastosowanie w inżynierii środowiska. Zeszyty Naukowe Instytu Gospodarki Surowcami Mineralnymi i Energią Polskiej Akademii Nauk, 102, 171–184.
8. Czuma, N. et al. 2019. Synthesis of zeolites from fly ash with the use of modified two-step hydrothermal method and preliminary SO_2 sorption tests. Adsorption Science and Technology, 37(1–2), 61–76.
9. Derkowski, A. et al. 2006. Properties and potential applications of zeolitic materials produced from fly ash using simple method of synthesis. Powder Technology, 166(1), 47–54.
10. Derkowski, A., Michalik, M. 2007. Statistical approach to the transformation of fly ash into zeolites. Mineralogia Polonica, 38(1), 47–69.
11. Feng, R. et al. 2019. Synthesis of ZSM-5 Zeolite Using Coal Fly Ash as an Additive for the Methanol to Propylene (MTP) Reaction. Catalyst, 9, 788.
12. Gollakota, A. et al. 2021. Coal bottom ash derived zeolite (SSZ-13) for the sorption of synthetic anion Alizarin Red S (ARS) dye. Journal of Hazardous Materials, 416, 125925.
13. He, P.Y. et al. 2020. Low-cost and facile synthesis of geopolymer-zeolite composite membrane for chromium(VI) separation from aqueous solution. Journal of Hazardous Materials, 392(13), 122359.
14. Hollman, G.G., Steenbruggen, G., Janssen-Jurkovičová, M. 1999. Two-step process for the synthesis of zeolites from coal fly ash. Fuel, 78(10), 1225–1230.
15. Hong, J.L.X. et al. 2017. Conversion of Coal Fly Ash into Zeolite Materials: Synthesis and Characterizations, Process Design, and Its Cost-Benefit Analysis. Industrial and Engineering Chemistry Research, 56(40), 11565–11574.
16. Hu, T. et al. 2017. Synthesis of zeolites Na-A and Na-X from tablet compressed and calcinated coal fly ash. Royal Society Open Science, 4(10), 170921.
17. Hui, K.S., Chao, C.Y.H. 2006. Effects of step-change of synthesis temperature on synthesis of zeolite 4A from coal fly ash. Microporous and Mesoporous Materials, 88(1–3), 145–151.
18. Inada, M. et al. 2005. Synthesis of zeolite from coal fly ashes with different silica-alumina composition. Fuel, 84(2–3), 299–304.
19. Król, M., Rożek, P., Mozgawa, W. 2017. Synthesis of the sodalite by geopolymerization process using coal fly ash. Polish Journal of Environmental Studies, 26(6), 2611–2618.
20. Kunecki, P. et al. 2017. Synthesis of faujasite (FAU) and tschernichite (LTA) type zeolites as a potential direction of the development of lime Class C fly ash. International Journal of Mineral Processing, 166, 69–78.
21. Kunecki, P. et al. 2018. Influence of the reaction time on the crystal structure of Na-P1 zeolite obtained from coal fly ash microspheres. Microporous and Mesoporous Materials, 266, 102–108.
22. Kunecki, P. et al. 2021. Influence of the fly ash fraction after grinding process on the hydrothermal synthesis efficiency of Na-A, Na-P1, Na-X and sodalite zeolite types. International Journal of Coal Science and Technology, 8(2), 291–311.
23. Kunecki, P., Panek, R., Wdowin, M. 2016. Na-P1 zeolite synthesis and its crystalline structure ripening through hydrothermal process using coal combustion by-products as substrates. Geology, Geophysics & Environment, 42(1), 90–91.
24. Kurniawan, R.Y. et al. 2018. Synthesis of Zeolite-X from Bottom Ash for H_2 Adsorption. IOP Conference Series: Materials Science and Engineering, 299, 012083.
25. Lankapati, H.M. et al. 2020. Mordenite-Type Zeolite from Waste Coal Fly Ash: Synthesis, Characterization and Its Application as a Sorbent in Metal Ions Removal. ChemistrySelect, 5(3), 1193–1198.
26. Liu, Y., Yan, C., Zhang, Z. 2016. A comparative study on fly ash, geopolymer and faujasite block for Pb removal from aqueous solution. Fuel, 185, 181–189.
27. Liu, Y., Yan, C., Qiu, X., et al. 2016. Preparation of faujasite block from fly ash-based geopolymer via in-situ hydrothermal method. Revista Mexicana de Urologia, 76(1), 433–439.
28. Missengue, R.N.M. et al. 2017. Transformation of South African coal fly ash into ZSM-5 zeolite and its application as an MTO catalyst. Comptes Rendus Chimie, 20(1), 78–86.
29. Musyoka, N.M. 2009. Hydrothermal synthesis and optimisation of zeolite Na-P1 from South African coal fly ash. M.Sc. Thesis, University of the Western Cape, Bellville.

30. Musyoka, N.M. et al. 2012. Optimization of hydrothermal synthesis of pure phase zeolite Na-P1 from South African coal fly ashes. Journal of Environmental Science and Health - Part A Toxic/Hazardous Substances and Environmental Engineering, 47(3), 337–350.
31. Padhy, R.R. et al. 2015. Ultrafine nanocrystalline mesoporous NaY zeolites from fly ash and their suitability for eco-friendly corrosion protection. Journal of Porous Materials, Springer US, 22(6), 1483–1494.
32. Pichór, W. et al. 2014. Synthesis of the zeolites on the lightweight aluminosilicate fillers. Materials Research Bulletin, 49(1), 210–215.
33. https://legislacja.gov.pl/projekt/12356300/katalog/12853158#12853158.
34. Ren, X. et al. 2020. Synthesis of zeolites from coal fly ash for the removal of harmful gaseous pollutants: A review. Aerosol and Air Quality Research, 20(5), 1127–1144.
35. Shabani, J.M. et al.2019. Synthesis of hydroxy sodalite from coal fly ash for biodiesel production from waste-derived maggot oil. Catalysts, 9(12), 1–14.
36. Sivalingam, S., Sen, S. 2018. Rapid ultrasound assisted hydrothermal synthesis of highly pure nanozeolite X from fly ash for efficient treatment of industrial effluent. Chemosphere, 210, 816–823.
37. Uliasz-Bocheńczyk, A., Mazurkiewicz, M. Mokrzycki, E. 2015. Popioły z energetyki – odpad, produkt uboczny, surowiec. Mineral Resources Management, 31(4), 139–150.
38. Um, N.I. et al. 2009. Immobilization of Pb, Cd and Cr by Synthetic NaP1 Zeolites from Coal Bottom Ash Treated by Density Separation. Resources Processing, 56(3), 130–137.
39. Uzarowicz, L., Zagorski, Z. 2015. Mineralogy and chemical composition of technogenic soils (Technosols) developed from fly ash and bottom ash from. Soil Science Annual, 66(2), 82–91.
40. Vilakazi, A.Q. et al. 2022. The Recycling of Coal Fly Ash: A Review on Sustainable Developments and Economic Considerations. Sustainability, 14(4), 1–32.
41. Wajda, A., Kozioł, M. 2015. Microspheres – acquisition, properties, applications. Inżynieria Środowiska, 1, 15–19.
42. Wałek, T.T., Saito, F., Zhang, Q. 2008. The effect of low solid/liquid ratio on hydrothermal synthesis of zeolites from fly ash. Fuel, 87(15–16), 3194–3199.
43. Wang, C.F. et al. 2008. Influence of NaOH concentrations on synthesis of pure-form zeolite A from fly ash using two-stage method. Journal of Hazardous Materials, 155(1–2), 58–64.
44. Wise, W.S. 2013. Zeolites. Reference Module in Earth Systems and Environmental Sciences, 1–11.
45. Woolard, C.D., Petrus, K., Van der Horst, M. 2000. The use of a modified fly ash as an adsorbent for lead. Water SA, 26(4), 531–536.
46. Xu, P. et al. 2017. Influence of Hg occurrence in coal on accuracy of Hg direct measurement based on thermal decomposition. International Journal of Coal Geology, 170, 14–18.
47. Zhou, T. et al. 2021. Organotemplate-free synthesis of MOR zeolite from coal fly ash through simultaneously effective extraction of Si and Al. Microporous and Mesoporous Materials, 314, 110872.
48. Zhu, M.H. et al. 2014. Structure directing agent-free synthesis of ZSM-5 zeolite membranes using coal fly ash as alumina source. Chemistry Letters, 43(6), 772–774.